

# A New Structural Modification Approach for Seismic Protection using Negative Stiffness Device



**D. T. R. Pasala & S. Nagarajaiah**

*Dept. of Civil and Environmental Engineering, Rice University, Houston, TX-77005, USA.*

**A. A. Sarlis, A. M. Reinhorn & M. C. Constantinou**

*Dept. of Civil and Envi. Engineering, University at Buffalo, Buffalo, NY-14260, USA.*

**D. Taylor**

*Taylor Devices Inc., North Tonawanda, NY-14120 U.S.A.*

## SUMMARY:

Yielding can be emulated in a structural system by adding an adaptive “negative stiffness device” (NSD) and shifting the “yielding” away from the main structural system-leading to the new idea of “apparent weakening” that occurs ensuring structural stability at all displacement amplitudes. This is achieved through an adaptive negative stiffness system (ANSS), a combination of NSD and a viscous damper. By engaging the NSD at an appropriate displacement (apparent yield displacement that is well below the actual yield displacement of the structural system) the composite structure-device assembly behaves like a yielding structure. The combined NSD-structure system presented in this study has a re-centering mechanism thereby avoids permanent deformation in the composite structure-device assembly unless, the main structure itself yields. Essentially, a yielding-structure is “mimicked” without any, or with minimal permanent deformation or yielding in the main structure. As a result, the main structural system suffers less accelerations, less displacements and less base shear, while the ANSS “absorbs” them. This paper presents comprehensive details on development and study of the ANSS/NSD. Through numerical simulations, the effectiveness and the superior performance of the ANSS/NSD as compared to a structural system with supplemental passive dampers is presented.

*Keywords: adaptive negative stiffness device (NSD); adaptive control; passive control; seismic protection*

## 1. INTRODUCTION

Conventional structures designed for loads specified by codes undergo significant inelastic deformations during severe earthquakes, leading to stiffness and strength degradation, increased interstory drifts, and damage with residual drift. These yielding structures however keep the global forces within limited bounds dictated by the yield strength (Reinhorn et al. 2002). The inelastic effects can be reduced substantially using passive seismic protection systems in the form of supplemental damping devices (Constantinou and Symans 1993; Spencer and Nagarajaiah 2003; Viti et al. 2006; Cimellaro et al. 2009). This approach has emerged as an efficient way to reduce response and limit damage by shifting the inelastic energy dissipation from the framing system to the dampers. Examples of few such passive systems are base isolation systems (Nagarajaiah 2009), fluid dampers (Constantinou and Symans 1993), tuned mass dampers (Nagarajaiah 2009).

Recently, Iemura and Pradono (2009) proposed pseudo-negative-stiffness dampers (PNSD) that are active or semi-active or hydraulic devices capable of producing negative-stiffness hysteretic loops. It has been shown in their investigations that by adding negative-stiffness hysteretic loops the total force would be lowered significantly. Common passive dampers that act in parallel with the stiffness of structure add to the total force rendering the shear force larger than that due to stiffness of the base-structure alone. A hydraulic device that is fully active, or semiactive, as in the case of PNSD Iemura and Pradono (2009) can generate a pseudo-negative stiffness in which case feedback control is needed to generate the negative stiffness. It must be noted that a passive hydraulic damper cannot “push” the structure in the same direction as the structural displacement; the adaptive negative stiffness device (NSD) proposed in this paper is designed to produce a true negative stiffness, however.

Combination of adaptive negative stiffness and damping device can result in reduction in base shear and displacement response of the structure. However, to date truly negative stiffness systems have received relatively little attention as compared to aforementioned semiactive or pseudo negative stiffness systems and thus represent a significant gap. Hence, development of new true negative stiffness devices is necessary to shift the yielding behavior from the structural system to ANSS/NSD.

### **1.1 Weakening and damping of structural systems**

Reinhorn et al. (2009) and Viti et al. (2006) introduced the concept of weakening structures (reducing strength), while introducing supplementary viscous damping to reduce simultaneously total accelerations and inter-story drifts. Design methodologies for changing the stiffness of structures and adding damping devices using control theory have been proposed by Gluck et al. (1999) to determine the magnitude and the locations of changed structural elements (often requiring softening rather than stiffening) and the added damping, while insuring structural stability. More recently, the design of weakened (reduced strength) structures with supplemental damping was introduced by Reinhorn et al. (2009), using principles of structural control. In the latter approach, a two-stage design procedure was suggested: (1) first using a nonlinear active control algorithm, to determine the new structural parameters while insuring stability, then (2) determine the properties of equivalent structural parameters of passive system, which can be implemented by removing, or weakening, some structural elements, or connections, reducing the yield capacity of the structure and by addition of energy dissipation systems. Passive dampers and weakened elements are designed using an optimization algorithm to obtain a response as close as possible to an actively controlled system. The weakening of structures leads to an early yielding of the structural system resulting in damage and permanent deformation. The idea of an “apparent weakening” is a new concept (ANSS) that is proposed in this study. An “apparent weakening” is introduced in the structural system using a complementary negative stiffness device (NSD) that mimics “yielding” of the global system thus attracting it away from the main structural system. Unlike the concept of weakening proposed earlier (summarized by Reinhorn et al., (2009)), where the main structural system strength is reduced, the new system does not alter the original structural system, but produces effects compatible with an early yielding.

Adaptive negative stiffness system (ANSS) refers to the assembly of NSD and passive damper (PD). It can also be simply referred as adaptive system or adaptive stiffness system. The main objective of the adaptive system is to shift the yielding behavior of the structure to the NSD and reduce the base shear (foundation force) of the structure and at the same time limit the maximum displacement and acceleration of structure. The two components of ANSS are designed in a two step sequence, similarly to the approach developed by Reinhorn et al. (2009). First an adaptive negative stiffness device, which is capable of changing its stiffness during lateral displacement, is developed based on the properties of the structure. This NSD is designed to exhibit negative stiffness behavior which upon the addition of structure properties will result in reduction of the stiffness of the structure and NSD assembly or “apparent weakening” there by resulting in the reduction of the base shear of the assembly. Then a passive damper is designed for the assembly to reduce the displacements that are caused due to the “apparent weakening”—there by reducing the base shear and displacement in a two step process.

## **2. NEGATIVE STIFFNESS DEVICE (NSD)**

True negative stiffness means that the force must assist motion, not oppose it as in the case of a positive stiffness spring. A negative stiffness device was developed by the authors. The detailed description of the device is presented by Apostolos et al. (2012), however, a shorter description of its development is included herein for sake of completeness. The schematic of the NSD is shown in Fig. 2.1(left). The NSD consists of a precompressed spring placed vertically between the two chevron braces CB1 and CB2, as shown in Fig. 2.1(left). It also has an elastic-bilinear spring placed horizontally, connecting CB2 and the bottom of the frame. Also, it is important to note that all vertical

forces generated by the precompressed spring are transferred to the double hinged column and will not be transferred to the structure (Sarlis et al. 2012). Since the precompressed vertical spring is connected to the braces CB1 and CB2 any interstorey displacement displaces the precompressed spring from its vertical position to an inclined position. The force exerted by the precompressed spring is amplified using a pivot plate and the braces (Pasala et al. 2012).

Force displacement characteristics of the vertical spring, horizontal spring and the NSD are shown in Fig. 2.1(right). Five distinct points are shown in Fig. 2.1(a). Point “0” is the initial position and lateral force exerted by the vertical spring,  $F_{vs}$ , is zero. When the precompressed vertical spring is displaced to an inclined position at angle  $\theta_s$  from the vertical, the axial force of the vertical spring,  $F_s$ , is given by

$$F_s = \left\{ P_{in} / K_s - (l_s - l_p) \right\} K_s \quad (2.1)$$

where  $K_s$  is the vertical spring stiffness,  $l_s$  is the length of the inclined spring,  $l_p$  is the length of vertical spring when  $u=0$ ,  $P_{in}$  is the initial compression force in the vertical spring. The horizontal component of the axial force,  $F_{vs}$ , that assists motion is given by

$$F_{vs} = \left( \frac{P_{in} + K_s l_p}{l_s} - K_s \right) \left( \frac{l_1}{l_2} \right) \left( 2 + \frac{l_2}{l_1} + \frac{l_p + l_1}{\sqrt{l_2^2 - u^2}} \right) u \quad (2.2)$$

where,  $l_1$  and  $l_2$  are the lengths of pivot plate. At point-“1” in Fig. 2.1(a) the secant stiffness ( $-F_{vs1}/u'_y$ ) and tangential stiffness (slope at point-“1”) are both negative. At point-“2” the secant stiffness ( $-F_{vs2}/u_2$ ) is still negative and tangential stiffness reaches zero. At point-“3” the secant stiffness ( $-F_{vs3}/u_3$ ) is still negative but the tangential stiffness becomes positive. At point-“4” secant stiffness becomes zero and the tangential stiffness remains positive. At point-“4”,  $l_s = l_p + P_{in}/K_s$ , hence the net axial force in the inclined spring becomes zero,  $F_s = 0$ , or all the precompression force is lost; thus  $F_{vs} = 0$ . At point-“5” both the secant stiffness and tangential stiffness are positive.

The horizontal spring exhibits elastic-bilinear behavior, the transition in stiffness occurs at displacement  $u'_y$  and stiffness of the spring is zero for  $|u| > u'_y$ , as shown in Fig. 2.1(b). The total force-displacement characteristics of the NSD is shown in Fig. 2.1(c). The initial stiffness of the horizontal spring,  $F_{g1}/u'_y$ , is designed to match (or be greater than) the initial negative stiffness of the inclined spring resulting in zero stiffness for the NSD till  $|u| < u'_y$  i.e.,  $F_{g1} - F_{v1} = 0$ . The stiffness of the horizontal spring,  $K_g$ , beyond  $u'_y$  is chosen to be zero (or a very low value); hence, essentially the behavior of vertical spring is reflected in the NSD for displacements beyond  $u'_y$ . NSD exhibits positive secant and tangential stiffness beyond point-“3”, as shown in Fig. 2.1(c). The force due to combination of inclined and horizontal spring,  $F_{NSD}$ , is given by

$$F_{NSD} = F_{vs} + F_{vs} = - \left( \frac{P_{in} + K_s l_p}{l_s} - K_s \right) \left( \frac{l_1}{l_2} \right) \left( 2 + \frac{l_2}{l_1} + \frac{l_p + l_1}{\sqrt{l_2^2 - u^2}} \right) u + K_g u \quad (2.3)$$

Where,  $K_g$  is horizontal spring stiffness that exhibits elastic bilinear behavior. Overall the NSD behaves like a *nonlinear-elastic spring* with variable stiffness as described above. The force displacement characteristics of the primary structure, NSD and the structure with NSD are shown in Fig. 2.1(d), (e) and (f) respectively. Primary structure is assumed to be bilinear inelastic, shown in Fig. 2.1(d). By adding an NSD to the primary structure the resulting force-displacement behavior of the combined system is shown in Fig. 2.1(f). The behavior of the structure with NSD will not be altered for  $|u| < u'_y$ .  $u'_y$  is called apparent yield displacement; beyond  $u'_y$  the stiffness of the combined system

drops down and remains close to zero till  $u_2$ . For displacements larger than  $u_2$  the combined systems exhibits stiffening behavior and at  $u_3$  the primary structure and the assembly (primary structure with NSD) will experience the same amount of force, shown in Fig. 2.1 (f). Beyond  $u_3$  the structure with NSD will have a very high stiffness and also has higher force compared to the primary structure. More detailed discussion on the working principle is given in the next section. The properties of vertical spring and nonlinear horizontal springs are chosen in such a way that the desired force displacement is achieved.

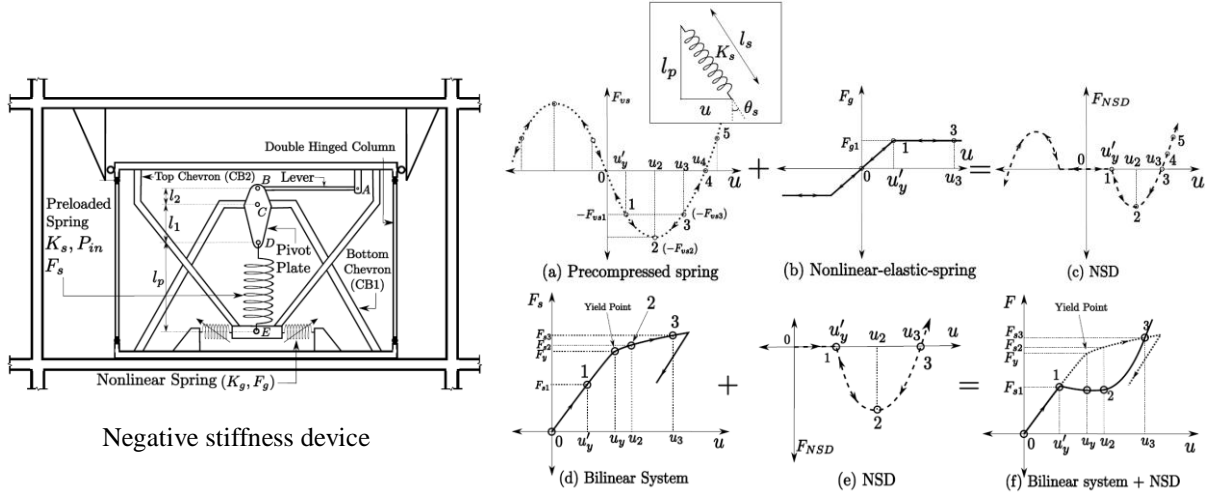


**Figure 2.1** (Left) Schematic diagram of the Negative Stiffness Device (NSD). (Right) Force displacement characteristics of component springs of NSD, primary structure and the assembly.

## 2.1 Working principle of ANSS

Assume a perfectly-linear single degree of freedom structure with stiffness,  $K_e$ , and no damping, an NSD with stiffness  $K_n$  and a passive damper with damping coefficient  $C$ . The force displacement plots are shown in Fig. 2.2 (a). By adding NSD to the structure, the assembly stiffness reduces to  $K_a = K_e - K_n$  beyond the displacement  $u'_y$  (shown in Fig. 2.2(b)). If,  $F_2$  and  $u_2$  are the maximum restoring force and maximum displacement of a perfectly-linear system then for the same load the maximum restoring force and maximum displacement of the assembly are  $F_3$  and  $u_3$ , respectively.  $K_n$  is designed to achieve the desired reduction in base shear. Force exerted by the NSD is shown in Fig. 2.2(b). Although the reduction in base shear is achieved the maximum deformation of adaptive system is substantially increased in the process when compared with an elastic system.

Deformation of this assembly can be reduced by adding a passive damping device in parallel to the NSD, shown in Fig. 2.2(c). By adding the viscous damper to the structure along with NSD, maximum displacement is reduced resulting in  $u'_3 < u_2$ . Since the assembly of structure and NSD acts like a nonlinear elastic system, viscous damper even with a small damping coefficient can be effective. It should be noted that by adding a damper to structure and NSD assembly, base shear of the assembly is not significantly increased. At this stage, there is one important constraint that is imposed on the NSD. From Fig. 2.2(a,b,c) it can be seen that there is an offset displacement,  $u'_y$ , called as ‘‘apparent yield-displacement’’, before the negative stiffness device is engaged. This is to avoid excessive response at relatively small external excitations. For displacements  $u$  such that  $|u| < u'_y$  the structure and NSD assembly behaves like the actual structure. This initial gap is provided by the horizontal spring with elastic-bilinear behavior that has been implemented using a pair of mechanical springs (Sarlis et al. 2011a).

The device and system is referred to adaptive because the behavior can be adjusted by varying the geometrical and mechanical properties. The device can be predesigned (adjusted/adapted) to exhibit different stiffnesses at different displacement ranges. For more detailed discussion on the challenges

involved in the application of NSD in inelastic structures readers should refer to Pasala et al. (2012).

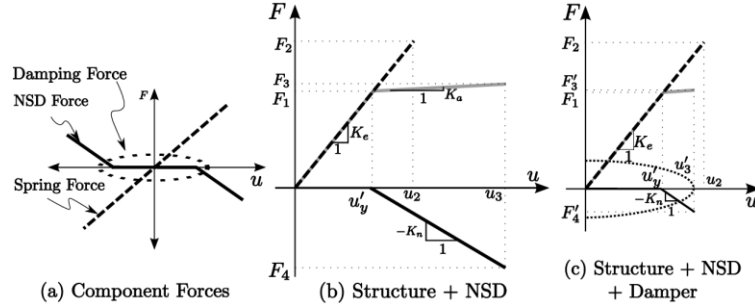


**Figure 2.2** Working principle of Adaptive system. [(dashed black line): Base-structure, (solid black line) : NSD, (grey line) : Assembly, (dotted black line) : Viscous damper]

So far, in this section, study on the desired characteristics of NSD was described. Since the NSD reduces the stiffness of the structure and the NSD assembly, increased deformations will result. To limit these deformations a passive damper has to be used. Assuming that we have the design ground motion for which the adaptive system has to be designed, the first step is to find the active control force exerted by the output feedback controller to satisfy desired performance specifications. Using optimization method proposed by Cimellaro et al. (2009) the optimal properties of the damper, that minimizes the error between the control force and force exerted by the passive devices, can be found. In this study, with the assumed NSD properties, a linear viscous damper with 20% damping ratio is found to be very effective. The damping force is  $F_{PD} = c\dot{u}$  and the effective damping due to the supplemental viscous fluid dampers is  $\xi = c / \left( 2\sqrt{K_{\text{tang}} m} \right)$ . The damping coefficient  $c$  is constant during either elastic or inelastic excursions. However the effective damping  $\xi$  is variable due to the variation of the tangential stiffness,  $K_{\text{tang}}$ . In particular,  $\xi$  becomes very large during the inelastic excursions. when the elastic excursions have low or zero post yield stiffness.

### 3. SIMULATION STUDIES

As mentioned in previous section the main objective of the adaptive system is to reduce the base shear (foundation force) of the structure and at the same time limit the maximum displacement and acceleration of structure. It will be uneconomical and unrealistic to design devices that will retain the structure in elastic state, without any yielding, after a major earthquake. So, all the cases considered in this paper involve structure whose properties are representative of a real building and the loading cases for which there is yielding in the structure.

Ultimate goal of this project is to experimentally prove the effectiveness of the proposed ANSS/NSD. All the simulation studies presented in this paper are for a 1:3 scaled three storey “zipper frame” like model structure developed at University at Buffalo, SUNY (Kusumastuti et al. 2005). In the initial phase 2<sup>nd</sup> and 3<sup>rd</sup> floors of the frame are braced. The capacity curve for the frame, obtained using the commercial softwares with the exact detailing, is shown in Fig. 3.1(left). The strength reduction factor of the three-story frame,  $R_{oy} = F_o / F_y = 1.25$ , which is a conservative design.  $F_o$  is the maximum force in the elastic system for the suite of the ground motions used in this study and  $F_y$  is the yield force of the three-story structure. The NSD is designed such that the strength reduction factor,  $R_{yy'} = F_y / F_{y'} = 4$ , where,  $F_{y'}$  is the apparent-yield-strength (force in the NSD and structure assembly at  $u_{y'}$ ). Hence, the NSD and structure assembly has a strength reduction factor,  $R_{oy'} = F_o / F_{y'}$  of 5. The strength reduction factor  $R_{yy'}$  should not be greater than 4 due to safety considerations. Sivaselvan-Reinhorn model (Sivaselvan and Reinhorn 2000) is used to capture the hysteretic behavior. Governing equation of motion for the structure is

$$m\ddot{u} + \left( 2\xi\sqrt{K_e m} \right) \dot{u} + \alpha K_e u + (1 - \alpha) K_e u_y z = -m\ddot{u}_g \quad (3.1)$$

$$dz/du = \left(1 - |z|^n (\gamma \times \text{sgn}(z \times du) + \beta)\right) / u_y \quad (3.2)$$

where,  $m$  is the mass of structure,  $\zeta$  is the damping ratio,  $\alpha$  is the post-yield stiffness ratio.  $\beta$ ,  $\gamma$  and  $\eta$  are constant parameters that determine the shape of bilinear hysteretic loops.  $z = F_{hys}/F_y$ , is the ratio of hysteretic force to the yield force. The values for remaining parameters are obtained using nonlinear interior-point optimization algorithm by minimizing the error between the capacity curve and the analytical model. The equation of motion for the adaptive system (combination of three-story structure, NSD and passive damper) is given by

$$m\ddot{u} + \left(2\xi\sqrt{K_e m}\right)\dot{u} + \alpha K_e u + (1-\alpha)K_e u_y z + F_{NSD} + F_{PD} = -m\ddot{u}_g \quad (3.3)$$

### 3.1 Simulation results: periodic ground motion

A periodic input consisting of five cycles sine function is used as an excitation with a frequency identical to the natural frequency of the base structure,  $\omega_n = \sqrt{K_e/m}$ . For those systems that will remain in elastic region for the design ground motion. NSD is found to be very effective. NSD will reduce the base shear of the structure substantially. To demonstrate this point, a periodic ground motion is applied to the frame. Amplitude of the ground motion is chosen such that the structure and NSD assembly will remain in elastic region. Response time histories comparing the actual structure and adaptive system are shown in Fig. 3.1(right). Adaptive system here refers to the structure, NSD and viscous damper with 0% damping. BS refers to base-structure (bilinear system) and ANSS refers to base-structure, NSD and damper (0%) assembly. It can be seen from results in Fig. 3.1(right) that all the response characteristics i.e., displacement, velocity and acceleration of the BS case have higher amplitude compared to the ANSS case. Force-displacement behavior of ANSS and BS is shown in Fig. 3.2(left) and the component forces acting in the ANSS are shown in Fig. 3.2(right). ‘‘Apparent yield displacement’’ for the NSD is assumed at a normalized displacement of 0.25. It is evident from the results in Fig. 3.2 that in the case of ANSS the primary structure remains in the elastic region (displacement of the ANSS is less than the yield displacement of the primary structure,  $u_y$ ), whereas in the case of base structure the primary structure yields. It should be noted that passive damper is not yet included for the results shown in Fig. 3.1(right) and Fig. 3.2. NSD alone is effective for reducing base shear, without any increased deformations, in elastic structures. A passive damper can be added to reduce the deformation of structure along with the base shear, which is considered next.

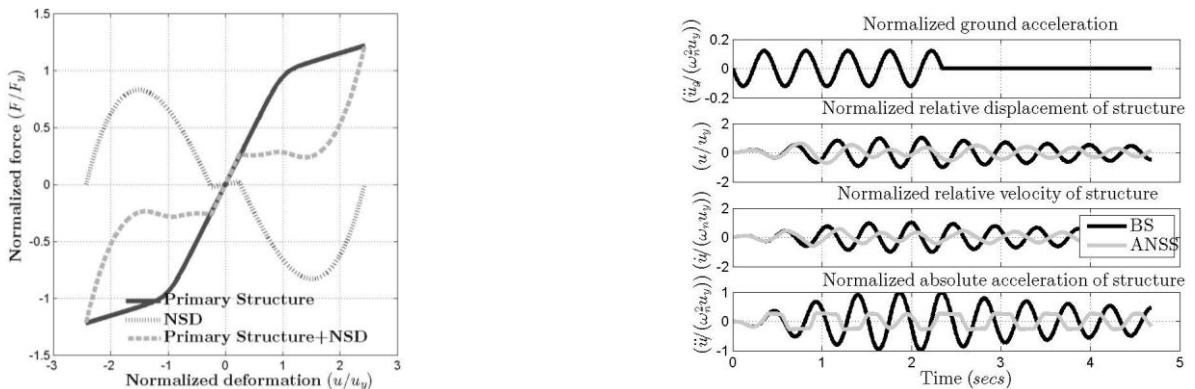


**Figure 3.1** (Left) Force-displacement behavior of base-structure, NSD and the assembly adapted for simulations. (Right) Comparison of responses of bi-linear system with and without NSD, in elastic region

The performance of the NSD is further verified for higher input amplitudes. Amplitude of input periodic ground motion is increased so that the adaptive system starts yielding. As discussed earlier, with NSD alone the deformation of the adaptive system will increase due to reduction of stiffness. Passive viscous damper with 20% damping ratio is used to contain the increased displacements that occur in the ANSS due to reduction in total stiffness of the system. Simulation results for three

systems are compared in Fig. 3.3, 3.4 after the addition of passive viscous damper: (i) Bilinear system (referred to as BS), (ii) Bilinear system with passive damper (referred to as PS) and (iii) Bilinear system with passive damper and NSD (referred to as ANSS). For all these systems response time histories are shown in Fig. 3.2(left), hysteresis loops and component forces are shown in Fig. 3.3(right) and Fig. 3.4(left) respectively. Structural spring force, damper force and NSD force in the adaptive system are shown in Fig. 3.4(right).

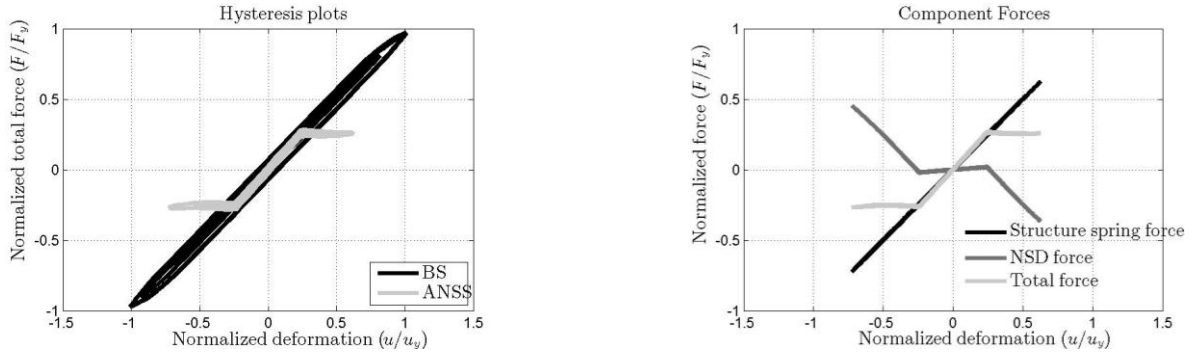


**Figure 3.2** (Left) Comparison of hysteresis plots of bi-linear system with and without NSD, in elastic region. (Right) Comparison of component spring forces in system with NSD, in elastic region

For the periodic input with input-frequency,  $\omega_n$ , and five cycles, the structure yields; the addition of passive damper results in the deformation of the structure being reduced substantially with a higher base shear. Fig. 3.3(left) shows the reduction in all the responses of an adaptive system (base-structure with NSD and passive damper). Maximum deformation of adaptive system and passive system are comparable in Fig. 3.4, but the acceleration of adaptive system is 40 % less--compared to passive system and base-structure. Forces exerted by the passive damper in case of both adaptive and passive system, shown in Fig. 3.4(left), are comparable. The shear forces experienced by the columns in the two cases of ANSS and PS are approximately the same, shown in Fig. 3.4(left). In the ANSS the base shear (force transferred to the structure's base) is reduced substantially, whereas in the PS case the base shear is larger than the BS case, shown in Fig. 3.4 Also, the accelerations reduce substantially in ANSS case, as compared to both BS and PS cases, which is a significant benefit as the secondary systems can be protected preventing sever post earthquake losses.

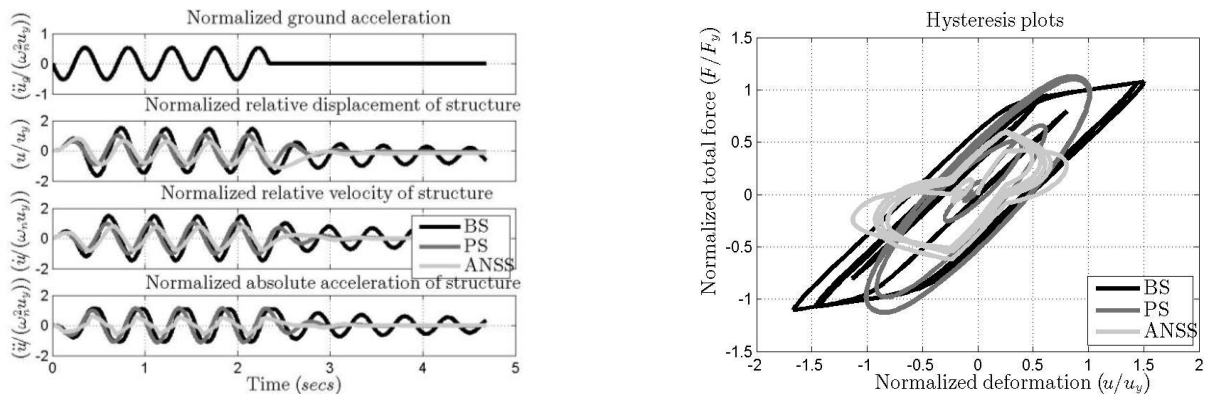


**Figure 3.3** (Left) Comparing responses for a yielding system with passive damper and NSD (BS, PS=BS+PD, ANSS=BS+PD+NSD). (Right) Comparing hysteresis loops for a yielding system with passive damper and NSD

### 3.2 Simulation results: earthquake ground motion

To demonstrate the efficiency of the ANSS for earthquake ground motions, four standard performance criteria suggested for nonlinear benchmark structures (Ohtori et al. 2004), are used to evaluate and compare the performance of ANSS with passively-controlled-structure and original structure.  $J_1$  is the performance index for inter-story deformation (normalized with the yield displacement),  $J_2$  is a measure of absolute story acceleration (normalized with the peak ground acceleration),  $J_3$  is the performance index for base shear, structure force with NSD force and PD force (normalized with the

yield force of the structure).  $J_4$  is the performance index for the force experienced by the columns of primary structure (normalized with the yield force of structure). Seven standard ground motions are used to evaluate the performance of the ANSS/NSD developed in this study. The performance indices of all the three systems for seven ground motions are listed in Table 3.1. From the results in Table 3.1, it can be seen that absolute accelerations ( $J_2$ ) of ANSS is lower than BS by 40% to 60% and it is lower than PS by 16% to 45%. Base shear ( $J_3$ ) of ANSS is lower than the BS by 55% to 70% and it is lower than PS by 40% to 65%. Inter-storey displacements ( $J_1$ ) of ANSS in some cases are 30% more than the PS but they are consistently less than BS by 20% or more. It should be noted that a simple viscous damper is adopted in these simulations. Better displacement reduction in ANSS can be achieved by finding the optimal linear/nonlinear damper properties for the given NSD properties. Although the base shear ( $J_3$ ) of the ANSS is lower than the PS by 55% or more, the force experienced by the columns ( $J_4$ ) follows the same trend as the inter-story displacement (shown in Table 3.1).

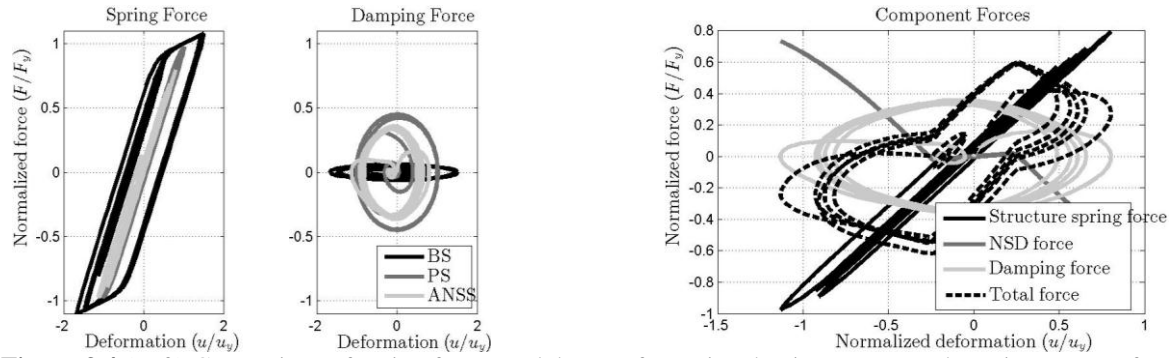


**Figure 3.4** (Left) Comparison of spring forces and damper forces in adaptive system and passive system, for a yielding system. (Right) Comparison of component forces in an adaptive system for large input amplitudes

Response characteristics of all the three systems (BS, PS and ANSS) for Sylmar fault-normal (FN) ground motion are shown in Fig. 3.5(left). Hysteresis loops and component forces of ANSS and PS for Sylmar FN ground motion is shown in Fig. 3.5(right). In the ANSS, when compared with PS, peak acceleration and base shear have been reduced by 40% for Sylmar FN excitation, shown in Fig. 3.5(right). Peak inter-storey deformation in the case of ANSS is 30% more than the PS and the peak damping force of ANSS is 35% less than the PS, shown in Fig. 3.5(right).

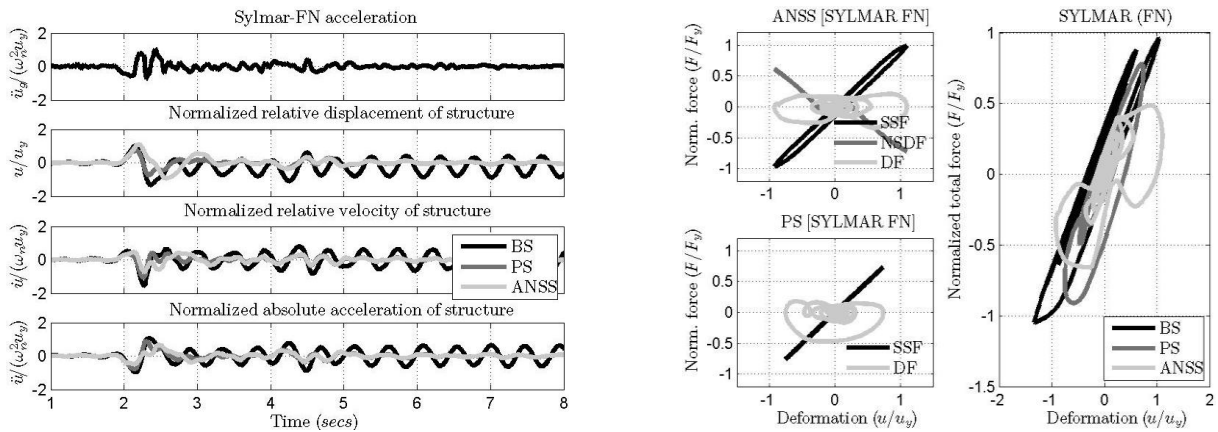


**Figure 3.5** (Left) Comparison of responses of base structure and passive system with adaptive system for Sylmar FN ground motion. (Right): Component forces of PS and ANSS; Force-displacement characteristics of base structure, passive system and adaptive system for Sylmar-FN ground motion.

To demonstrate that the proposed adaptive negative stiffness device is effective for a range of structural systems (systems with different natural frequencies) response spectra are generated for BS, PS and ANSS. The responses are presented in dimensionless  $\pi$ -terms, displacement  $(u(\omega_p)^2)/a_p$ , base shear  $-F_{shear}/(m a_p)$ , acceleration  $-\ddot{u}/a_p$  and frequency  $-T_s/T_p$ . Where,  $a_p$  is the pulse-amplitude of the acceleration,  $\omega_p$  is the frequency of the pulse,  $T_s$  and  $T_p$  are the time-periods of structure and pulse,

respectively. Makris and Black (2004) have developed cycloidal pulses that are representative of the actual recorded ground motions. These cycloidal pulses and recorded ground motion data are used to test the performance of the ANSS. Response spectra are generated for both cycloidal pulses and recorded ground motions. Response-spectra plots are represented in dimensionless  $\pi$ -terms proposed by Makris and Black (2004). All the earthquake motions responses are represented by equivalent pulses and the corresponding amplitudes and time-periods for normalization. Response spectra of  $C_1$  pulse type ground motion and Sylmar FN ground motion are shown in Fig. 3.6, respectively. For  $C_1$  ground motion, the pulse-period,  $T_p=0.5$  secs is used to generate spectra in Fig. 3.6(left). The Sylmar FN ground motion can be approximated by a  $C_2$  pulse with a period ( $T_p$ ) of 2.3 seconds and an acceleration peak ( $a_p$ ) of 64.6 in/sec<sup>2</sup>, which is used to normalize the spectra in Fig. 3.6(right).

For highly stiff structures the response of the PS and ANSS are similar because the normalized displacement of the structure remains less than 0.25, shown in Fig. 3.6(right) (top-left). For time-period of structure,  $T_s$ , greater than the pulse time-period,  $T_p$ , ( $T_s/T_p > 1$ ) peak acceleration and base shear of the ANSS is substantially lower than BS and PS because of the NSD, shown in Fig. 3.6(top-right and bottom-right). For  $T_s/T_p > 3$ , all the three systems (BS,PS and ANSS) start yielding and the NSD starts stiffening so the peak acceleration and base shear of all the systems are same, shown in Fig. 3.6(top-right and bottom-right). Column force in the ANSS is slightly higher than the PS around the peak in the spectra plots and it is almost identical for all other time-periods. Peak relative displacement of BS is always greater than the PS and ANSS.

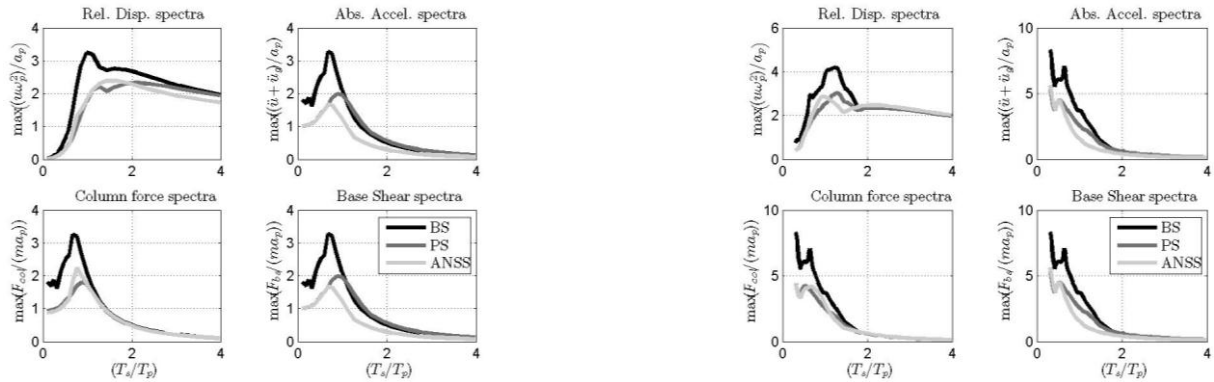


**Figure 3.6** (Left) Comparison of response spectra for cycloidal pulse type  $C_1$ . (Right) Comparison of response spectra for Sylmar FN ground motion.

**Table 3.1** Summary of results for seven recorded ground motions

GM	$J_1$			$J_2$			$J_3$			$J_4$		
	BS	PS	ANSS									
Elcentro #5 FN	0.72	0.48	0.64	4.01	2.83	2.3	0.72	0.48	0.29	0.72	0.48	0.64
Lucerne Valley FN	0.98	0.47	0.69	7.86	4.19	3.52	0.93	0.47	0.28	0.93	0.47	0.69
Rinaldi	1	0.64	0.83	2.9	2.05	1.36	0.97	0.64	0.3	0.97	0.64	0.82
Erzincan	0.68	0.45	0.56	3.42	2.41	1.96	0.68	0.45	0.27	0.68	0.45	0.56
Newhall	1.66	0.93	0.93	1.81	1.63	0.99	1.1	0.9	0.31	1.1	0.9	0.9
Sylmar	1.24	0.65	0.78	6.46	4.79	2.66	1.03	0.65	0.3	1.03	0.65	0.78
Pacoima	0.61	0.45	0.55	2.3	1.81	1.4	0.61	0.45	0.27	0.61	0.45	0.55

#### 4. CONCLUSIONS

The adaptive negative stiffness system proposed in this paper consists of two elements: 1) a true negative stiffness device (NSD) and 2) a passive damper (PD). Upon the addition of NSD to the structural system, predesigned reductions of stiffness occur in the combined system or “apparent softening and weakening” occurs; however, it is important to note that the stiffness and the strength of

the main structural system remain unchanged in this study (hence, “apparent”). Addition of the passive damper reduces effectively the displacements that are caused due to the reduction in effective stiffness. Effectiveness of the proposed ANSS/NSD in elastic and inelastic structural systems has been demonstrated through the simulation studies for both periodic and random input ground motions. Key conclusions of these numerical studies are (1) for structures that remain in the elastic range NSD reduces the base shear substantially, (2) if deformations increase inadvertently or a controlled reduction in deformation is also a criterion, then adding a passive damper with nominal damping coefficient achieves the goal, and (3) for yielding structures, appropriate combination of NSD and passive damper significantly reduces deformations, accelerations, and base shear. In the case with ANSS the base shear (forces experienced by the foundation) is reduced substantially, whereas in the PS case the base shear is larger than the BS case. The shear forces experienced by the columns in the two cases of ANSS and PS is approximately the same, but substantial reduction in accelerations occur in ANSS case as compared to both BS and PS cases-which a significant benefit as the secondary systems can be protected from severe post earthquake losses. In summary, the main structural system suffers less accelerations, less displacements and less base shear or force at the foundation level, while the ANSS “absorbs” them.

## ACKNOWLEDGEMENTS

Funding by National Science Foundation, grant NSF-CMMI--NEESR-0830391 for this project with Dr. Joy Pauschke as program director is gratefully acknowledged.

## REFERENCES

- Cimellaro, G. P., Lavan, O., and Reinhorn, A. M. (2009). “Design of passive systems for control of inelastic structures.” *Earthquake Engineering & Structural Dynamics*, **38(6)**, 783–804.
- Constantinou, M. C., and Symans, M. D. (1993). “Experimental study of seismic response of buildings with supplemental fluid dampers.” *The Structural Design of Tall Buildings*, **2(2)**, 93–132.
- Gluck, N., Reinhorn, A. M., Gluck, J., and Levy, R. (1999). “Design of supplemental dampers for control of structures.” *Journal of structural Engineering*, **122(12)**, 1394.
- Iemura, H., and Pradono, M. H. (2009). “Advances in the development of pseudo-negative-stiffness dampers for seismic response control.” *Structural Control and Health Monitoring*, **16(7-8)**, 784–799.
- Kusumastuti, D. K., Reinhorn, A. M., and Rutenberg, A. (2005). *A Versatile Experimentation Model for Study of Structures Near Collapse Applied to Seismic Evaluation of Irregular Structures*. Report MCEER-05-0002, SUNY/Buffalo.
- Makris, N., and Black, C.J. (2004). “Dimensional analysis of rigid-plastic and elastoplastic structures under pulse-type excitations.” *Journal of engineering mechanics*, **130(9)**, 1006-1018.
- Nagarajaiah, S. (2009). “Adaptive passive, semiactive, smart tuned mass dampers: identification and control using empirical mode decomposition, hilbert transform, and short-term fourier transform.” *Structural Control and Health Monitoring*, **16(7-8)**, 800–841.
- Ohtori, Y., Christenson, R., Spencer Jr, B. F., and Dyke, S. J. (2004). “Benchmark control problems for seismically excited nonlinear buildings.” *Journal of Engineering Mechanics*, **130(4)**, 366-385.
- Pasala, D.T.R., Sarlis, A.A., Nagarajaiah, S., Reinhorn, A.M., Constantinou, M.C. and Taylor, D. (2012). “A new structural modification approach for seismic protection of structures”, *J. of Str. Engineering*, (accepted for publication, March 2012).
- Reinhorn, A. M., Lavan, O., and Cimellaro, G. P. (2009). “Design of controlled elastic and inelastic structures.” *Earthquake Engineering and Engineering Vibration*, **8(4)**, 469–479.
- Sarlis, A.A., Pasala, D.T.R., Constantinou, M.C., Reinhorn, A.M., Nagarajaiah, S., and Taylor, D. (2012). “Negative stiffness device for seismic protection of structures” *J. of Str. Engineering*, (accepted for publication, March 2012).
- Sivaselvan, M. V., and Reinhorn, A. M. (2000). “Hysteretic models for deteriorating inelastic structures.” *Journal of Engineering Mechanics*, **126(6)**, 633–640.
- Spencer, B. F., and Nagarajaiah, S. (2003). “State of the art of structural control.” *Journal of Structural Engineering*, **129**, 845-856.
- Viti, S., Cimellaro, G. P., and Reinhorn, A. M. (2006). “Retrofit of a hospital through strength reduction and enhanced damping.” *Smart Structures and Systems*, **2(4)**, 339–355.